Molten salt preparation of K–Zr ternary phosphates

A. V. Barabanova,[a] A. O. Turakulova,[a] V. V. Lunin[a] and P. Afanasiev*[b]

[a]*Moscow State University, Chemistry Department, Moscow, 119899, Russia*

[b]*Institut de Recherches sur la Catalyse, 2 Avenue A. Einstein, 69626, Villeurbanne, Cédex, France*

Mixed phosphates of K and Zr have been prepared by means of the reactions of hydrated $ZrOCl_2$ and $NH_4H_2PO_4$ salts with KNO_3 in the temperature range 250–550 °C. Molten salt reactions were studied by thermogravimetry and mass spectrometry of the evolved gases. Thermal analysis of the ternary mixture demonstrated that a strongly exothermic mass loss occurs at *ca.* 250 °C, due to the reaction producing a $KHZr(PO_4)_2$ phase. Depending on the reaction conditions, different solids can be obtained, including dispersed zirconia superficially doped with phosphate or crystalline ternary phosphates such as $KZr_2(PO_4)_3$ of NASICON structure or the layered compound $K_2Zr(PO_4)_2$. The solids obtained were characterized by X-ray diffraction, ^1H and ^{31}P NMR spectroscopy. A correlation of ^{31}P chemical shift and the mean electronegativity of the obtained solids has been proposed.

Molten nitrates as reaction media provide some original possibilities for the preparation of solid materials. Reactions in molten nitrates have been utilized for the preparation of finely divided oxides for applications in ceramics or catalysis. Highly dispersed oxides of Zr, Al or Ti have been obtained by the reactions of the mixtures of the corresponding metal salts with the alkali-metal nitrates.[1–3] In such syntheses molten nitrates react as oxobases (Lux–Flood bases), *i.e.* they donate an oxide ion to any appropriate electrophilic species, causing precipitation of an oxide (that of Mg, Al, Ti, Zr) or formation of some soluble oxoanions (SO_4^{2-}, MoO_4^{2-}).

If the nitrate melts are doped with polyvalent oxoanions like sulfate, phosphate or molybdate, interactions between the oxoanions and other metal species can lead to various products such as fine dispersions similar to the supported catalysts (molybdate species on zirconia[4]) or complex ternary and quaternary salts, for example calcium chromate.[5]

Few works deal with the chemistry of phosphates in the nitrate melts. Solubility of alkali-metal phosphates in molten nitrates and the acidobasic transformations of phosphate ions in molten nitrate have been reported earlier.[6–8] Ion exchange isotherms of α-Zr phosphate in different nitrate melts have been obtained.[9–11] However, chemical reactions of phosphate and transition-metal species in the nitrate melts were never studied.

Ternary and more complex phosphates including Zr possess physicochemical properties interesting for applications as ion exchangers,[12] high-temperature ion conductors,[13] catalysts[14,15] and non-linear optics materials.[16]

Recently, the possibility of forming ternary zirconium–alkali-metal phosphates in K–Na low-melting point mixtures has been reported,[17] which opens a new soft chemistry route for the preparation of these important solids. The present work deals with the study of the reactions of zirconium and phosphate species in the KNO_3 melt and the characterization of its solid products.

Experimental

Preparation of solids

Zirconium oxychloride octahydrate, ammonium hydrophosphate $NH_4H_2PO_4$ and potassium nitrate (all Aldrich ACS reagents) were employed as the reactants. The reaction was carried out in a glass reactor under a nitrogen flow. Dehydration at 150 °C for 2 h and reaction at 250–550 °C for 2 h were subsequently carried out (unless otherwise stated). After the reaction, the insoluble product was extracted at room temperature from the solidified melt by distilled water, then dried in air at 100 °C for 24 h. Some samples of the solidified melts were taken directly for the characterizations. In the reaction mixtures the atomic ratio P/Zr varied from 0.1 to 10. Potassium nitrate was always taken in a tenfold molar excess relative to the amount of Zr salt.

Study of the reaction products

The reaction was studied using a mass spectrometer Gas trace A (Fisons Instruments) equipped with a quadrupole analyser (VG analyser) working in a Faraday mode. Mixtures containing *ca.* 1 g of salts were heated in a glass cell with a heating rate of 1.5 °C min^{-1} from room temperature to 550 °C. A silica capillary tube heated at 180 °C continuously bled off gaseous reaction products. Signals were registered with *m*/*z* 15, 18, 30, 32, 36, 44, 46, corresponding respectively to NH (from NH_3), H_2O, NO, O_2, HCl, CO_2 and NO_2. Thermogravimetric measurements were carried out using a Paulik D1500 device in the platinum crucibles in air, the heating parameters being the same as in the mass spectrometric study. X-Ray diffractograms (XRD) were recorded on a Siemens D500 diffractometer using Ni-filtered Cu-Kα radiation. Standard files of JCPDS were employed to identify the phases. Simulation of powder XRD patterns was made using the Powder Cell 1.8 program.[18] Surface areas and pore radii distributions were measured by nitrogen adsorption. ^{31}P and ^1H NMR spectra were obtained on a Bruker MSL 300 device. MAS spectra (*ca.* 3.5 KHz) were registered with the proton decoupling of the ^{31}P signal. Chemical analyses of phosphorus, zirconium and alkali metals were carried out using an atomic emission method with a spectroflame ICPD device.

Results and Discussion

Reactions of the precursor compounds and their mixtures (DTA–DTG and MS data)

Since in the system $ZrOCl_2$–KNO_3–$NH_4H_2PO_4$ all the components can react with each other, understanding of the ternary system can be strongly assisted by comparison with the reactions of simpler binary mixtures and/or decomposition of the individual precursor compounds. Therefore some of the DTA–DTG and MS data are presented below for binary mixtures.

$ZrOCl_2 + KNO_3$. Decomposition of $ZrOCl_2 \cdot 8H_2O$ in air commences at rather low temperature (*ca.* 100 °C) and above *ca.* 370 °C leads to the formation of crystalline ZrO_2.[19] While heating $ZrOCl_2 \cdot 8H_2O$ in air, endothermic peaks due to dehydration at 130 and 160 °C are followed by the progressive mass decrease up to 500 °C, without any thermal events. Mass spectrometric data show that after elimination of water, the only gaseous product is HCl. The mass loss observed at 530 °C was 59.1%; the calculated value for the reaction (1) is 61.5%.

$$ZrOCl_2 \cdot 8H_2O \rightarrow ZrO_2 + 7H_2O + 2HCl \quad (1)$$

Differential thermal analysis of the $ZrOCl_2 \cdot 8H_2O$ reaction with the low-melting point $NaNO_3$–$KaNO_3$ mixture has been discussed earlier,[19] whereas here we used individual KNO_3. Compared to the $NaNO_3$–KNO_3 mixture, the curve in pure KNO_3 differs by the absence of distinct reaction peaks in the high temperature domain (Fig. 1). The endothermic events are the dehydration of zirconium salt (at 100 °C), the α–β transition in solid KNO_3 (140 °C) and its melting (334 °C). The smearing of the mass loss over the temperature scale seems to be related to the higher melting point of KNO_3 (334 °C). Apparently, at the moment of KNO_3 melting a significant amount of the zirconium oxychloride is already decomposed. The observed mass loss (68%) is intermediate between the value observed for $ZrOCl_2 \cdot 8H_2O$ decomposition and calculated for the reaction (2) (78%):

$$ZrOCl_2 + 2KNO_3 \rightarrow ZrO_2 + 2NO_2 + 1/2O_2 + 2KCl \quad (2)$$

The mass spectrum of the same (preliminary dehydrated at 100 °C) mixture is shown in Fig. 2. It corresponds to eqn. (2) above 300 °C but there is no production of oxygen at lower temperatures. At the same time strong peaks of NO and NO_2 appeared at 180 °C (NO_2 gas gives the signals of m/z 30 and 46 with an intensity ratio of 10, as observed elsewhere[20]). It can be explained by the reaction with the impurity of highly reactive nitrite, always present in the commercial nitrate [eqn. (3)].

$$ZrOCl_2 + 2KNO_2 \rightarrow ZrO_2 + NO_2 + NO + 2KCl \quad (3)$$

On the basis of the observed DTA–DTG and MS data, it can be stated that the reaction of hydrated $ZrOCl_2$ in KNO_3 occurs as a superposition of reactions (1)–(3). The solid product obtained at 500 °C is dispersed ZrO_2 as discussed in ref. 19. Note that the H_2O curve of the mass spectrum does not coincide with the dehydration maximum in Fig. 1 since the mixtures taken for MS study were dried at 100 °C in an oven overnight, to avoid the presence of water which tends to condense in the capillary and block it.

$NH_4HPO_4 + KNO_3$. On the DTA–DTG curves of this binary mixture (Fig. 3), dehydration of ammonium salt with the endothermic mass decrease is seen (190, 250 °C); then an endothermic mass loss appears at 350 °C. No events occur between 350 and 500 °C. Two narrow mass losses at 525–530 °C and 580–600 °C were observed, having opposite thermal effects.

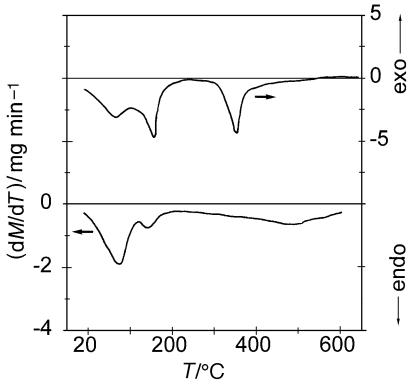

Fig. 1 Thermal analysis curves of the reaction of $ZrOCl_2 \cdot 8H_2O$ (32 mg) with KNO_3 (100 mg)

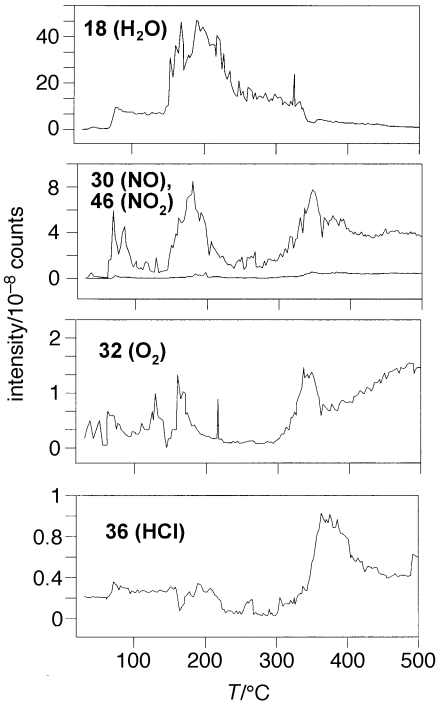

Fig. 2 Mass spectra of gases evolved in the reaction of $ZrOCl_2 \cdot 8H_2O$ (32 mg) with KNO_3 (100 mg)

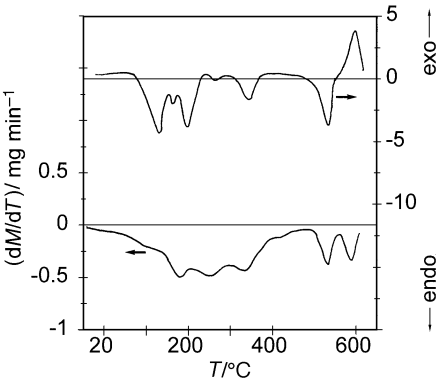

Fig. 3 Thermal analysis curves of the reaction of $NH_4H_2PO_4$ (60 mg) with KNO_3 (200 mg)

XRD data show that the solidified melt after the reaction at 350 °C contained a large amount of potassium metaphosphate KPO_3 whereas that after 550 °C contained orthophosphate K_3PO_4 and some pyrophosphate $K_4P_2O_7$. Therefore, the mass loss at 350 °C can be related to the reaction of the ammonium salt with the nitrate yielding KPO_3 [eqn. (4)], whereas the high temperature peaks are due to the further acid–base reactions leading to the orthophosphate.

$$NH_4H_2PO_4 + KNO_3 \rightarrow KPO_3 + NO + 1/2N_2 + 3H_2O \quad (4)$$

$$KPO_3 + 2KNO_3 \rightarrow K_3PO_4 + 2NO_2 + 1/2O_2 \quad (5)$$

The presence of $K_4P_2O_7$ in the reaction products and two equal peaks on the DTG curve allow us to conclude that reaction (5) is in fact the sum of two steps:

$$2KPO_3 + 2KNO_3 \rightarrow K_4P_2O_7 + 2NO_2 + 1/2O_2 \quad (6)$$

$$K_4P_2O_7 + 2KNO_3 \rightarrow 2K_3PO_4 + 2NO_2 + 1/2O_2 \quad (7)$$

The mass spectra of gaseous products are presented in Fig. 4. Ammonia produced at low temperatures obviously comes from

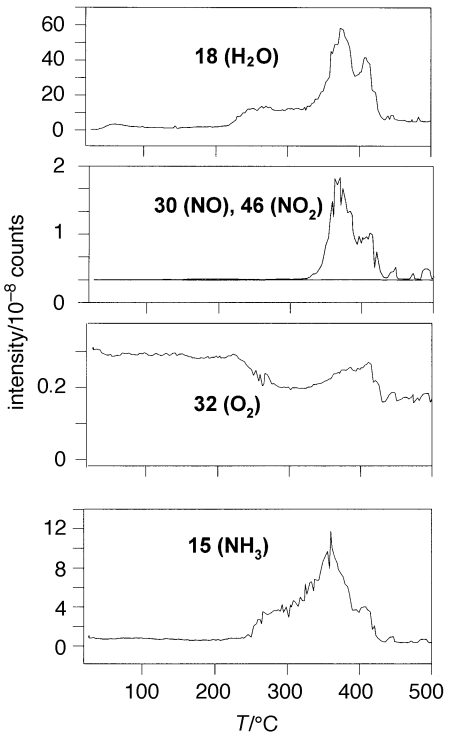

Fig. 4 Mass spectra of gases evolved in the reaction of $NH_4H_2PO_4$ (60 mg) with KNO_3 (200 mg)

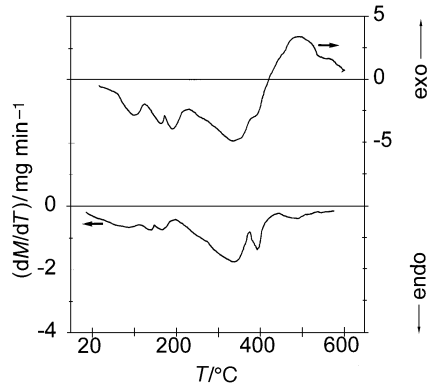

Fig. 5 Thermal analysis curves of the reaction of $NH_4H_2PO_4$ (120 mg) with $ZrOCl_2 \cdot 8H_2O$ (64 mg)

the decomposition of the ammonium salt. Large amounts of water and nitrogen oxide at *ca.* 350 °C are produced apparently by the reaction (4). Only the beginning of NO_2 formation due to the reactions (6) and (7) could be observed in the glass reactor used for the MS studies.

$NH_4H_2PO_4 + ZrOCl_2$. Thermal analysis (Fig. 5) showed an exothermic process widely spread over the temperature range. The mass loss measured at 500 °C for the mixture of atomic ratio P/Zr = 2 was 52.5%; the calculated value for reaction (8) is 51.9%.

$$2NH_4H_2PO_4 + ZrOCl_2 \cdot 8H_2O \rightarrow ZrP_2O_7 + 2NH_4Cl(g) + 10H_2O \quad (8)$$

The water-insoluble product obtained at 500 °C for the mixtures of P/Zr ratio of 2, 4 or 10 consisted of pure crystals of ZrP_2O_7 (JCPDS card 24-1490). No MS study has been carried out for this reaction.

$NH_4H_2PO_4 + ZrOCl_2 + KNO_3$. The most important difference appearing in the thermal analysis curves of the ternary mixture compared to any of the binary mixtures is a strong exothermic effect at *ca.* 250 °C, with a narrow peak of mass loss in the DTG curve (Fig. 6). Since the event at 250 °C was found only in the ternary mixture, it must relate to a reaction of all the three compounds composing the ternary mixture. This reaction cannot be classified as a Lux–Flood interaction, because the amounts of oxygen and nitrogen oxides evolved at 250 °C are very small (Fig. 7). We suggest that it is a metathetical reaction which occurs due to a strong affinity of phosphate for the Zr species. At 240–250 °C the reaction mixture remains solid though it strongly sinters. XRD of the mixture after heating at 250 °C showed the appearance of $KHZr(PO_4)_2$ crystals (JCPDS card 28-0759, Fig. 8), so that

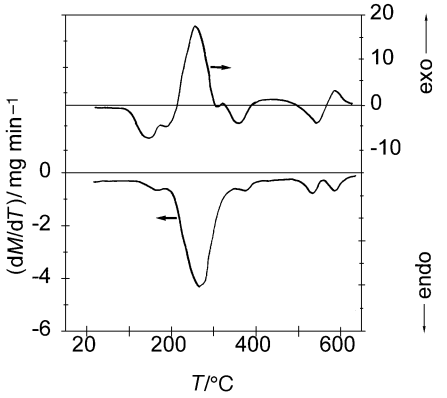

Fig. 6 Thermal analysis curves of the reaction of the ternary mixture of $NH_4H_2PO_4$ (60 mg) with $ZrOCl_2 \cdot 8H_2O$ (32 mg) and KNO_3 (400 mg)

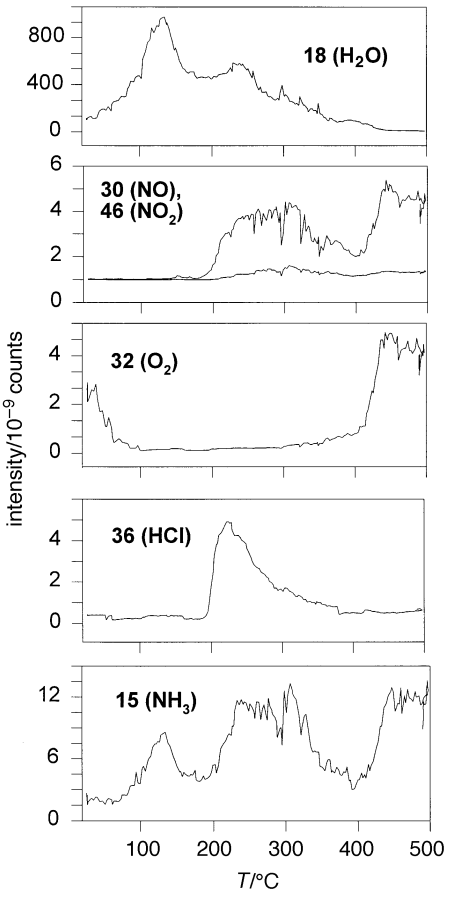

Fig. 7 Mass spectra of gases evolved in the reaction of the ternary mixture of $NH_4H_2PO_4$ (15 mg) with $ZrOCl_2 \cdot 8H_2O$ (8 mg) and KNO_3 (100 mg)

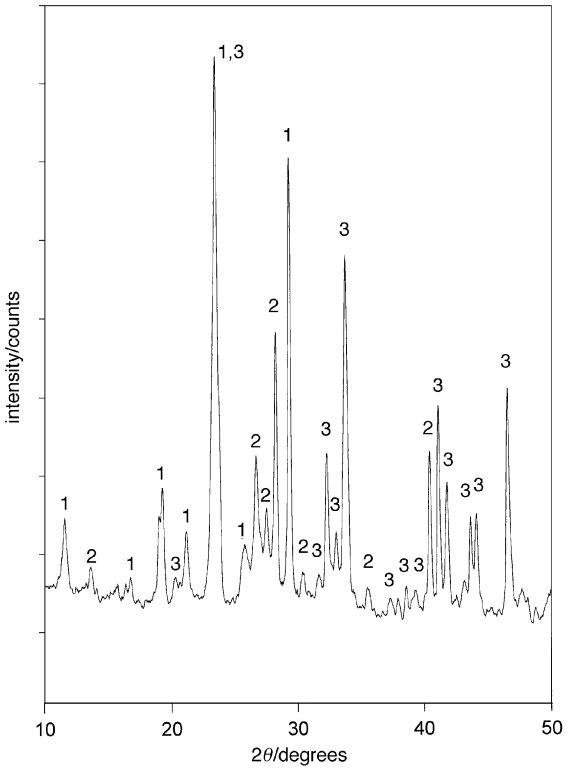

Fig. 8 XRD pattern of the ternary reaction mixture KNO_3–$NH_4H_2PO_4$–$ZrOCl_2 \cdot 8H_2O$ heated at 250 °C for 1 h. Peak 1, $KHZr(PO_4)_2$ (JCPDS 28-0759); 2, KPO_3 (JCPDS 43-0099); 3, KNO_3 (JCPDS 5-0377).

eqn. (9) can be written to explain the solid and gaseous products observed.

$$2NH_4H_2PO_4 + ZrOCl_2 \cdot 8H_2O + KNO_3 \rightarrow KHZr(PO_4)_2 + 2HCl + 4H_2O + 1/3NH_3 + 4/3N_2 \quad (9)$$

Reaction (9) is the simplest one including all the reactants and the products; it does not have any mechanistic value. Side reactions are of course possible, including decomposition of salts and(or) the binary reactions discussed above. Some $KZr_2(PO_4)_3$ phase with the NASICON structure (JCPDS card 35-0756) was observed in the mixture after heating at 270 °C [eqn. (10)]. NASICON becomes the only reaction product at 350 °C. It is likely that NASICON was produced from the decomposition of zirconium–potassium hydrogen phosphate.[21,22]

$$2KHZr(PO_4)_2 \rightarrow KZr_2(PO_4)_3 + KPO_3 + H_2O \quad (10)$$

At higher temperatures, the mass spectra and DTG curves of the ternary mixture containing excess of phosphate almost coincide with those of the binary $NH_4H_2PO_4 + KNO_3$ mixture, showing the transformation of KPO_3 to K_3PO_4 independently of the reactions of the Zr compounds. The XRD study shows that beginning from 400 °C the NASICON phase gradually transforms to the layered phosphate $K_2Zr(PO_4)_2$ though no distinct features in the thermal analysis curves or in the mass spectra can be related to this transformation. The reaction producing the layered phase can be formally written as the addition to the latter of orthophosphate, without the production of any gases [eqn. (11)].

$$KZr_2(PO_4)_3 + 3K^+ + PO_4^{3-} \rightarrow 2K_2Zr(PO_4)_2 \quad (11)$$

Further enrichment of the Zr-containing product with phosphate or(and) potassium never occurred for the conditions applied. $K_5Zr(PO_4)_3$ phase could not be obtained even at 550 °C and P/Zr = 10.

Some remarks should be made concerning the identification of the layered phase. Though the XRD pattern obtained could be perfectly indexed as an individual hexagonal phase with $a = 5.716$ Å and $c = 9.012$ Å, no identification with the JCPDS catalogue was possible. However, the best fit was obtained with the JCPDS card 45-232 for $K_2Zr(PO_4)_2$.[23] All the lines fitted except for a strong line at $d = 4.004$ Å in our pattern and one at $d = 3.735$ Å in ref. 23. Probably, there is an error in the article and consequently in the JCPDS card. The structure determination of the anhydrous $K_2Zr(PO_4)_2$ monocrystal has been done earlier.[24] This phase possesses a layered structure and crystallizes in the space group $P\bar{3}$. However, no powder diffractogram has been reported in ref. 24. Taking the atomic coordinates from ref. 24, we simulated the XRD pattern using the Powder Cell program.[18] Calculated XRD peaks positions and intensities coincided with those observed by us experimentally.

Note also that metaphosphate and pyrophosphate ions are present in the melt as the intermediate products in the course of reaction, but there are no signs of their interaction with Zr species. Apparently, since these anions are less basic than orthophosphate, the stability of their complexes with Zr^{IV} is lower.

Solid products of the ternary reaction $NH_4H_2PO_4 + ZrOCl_2 + KNO_3$ as a function of temperature and P/Zr ratio

Here are presented the results of the characterization of the products obtained by water extraction from the solidified melts. As follows from the chemical analyses, all the Zr loaded in the reaction mixtures was found in the precipitates, whatever the reaction conditions were. No Zr species was found in the washing solutions. Unless otherwise stated the solids were characterized after thorough washing with distilled water and oven drying at 120 °C. The properties of the solids *vs.* the reaction temperature and the P/Zr ratio are listed in Table 1.

The ratios P/Zr from 0.1 to 10 have been studied for the reaction temperatures 350 °C (samples 1–4) or 500 °C (samples 5–9). Chemical analyses show a tendency of phosphate to be bound within the water-insoluble solid, even if no crystalline Zr phosphates are formed (P/Zr = 0.1). Since the samples 1 and 5 contained only the ZrO_2 phase (Fig. 9) we suppose that in these samples phosphate groups are anchored on the surface of the dispersed zirconia.

Increase of the specific surface area of zirconia due to the phosphate admixture is observed (200 $m^2\ g^{-1}$, sample 5), compared to that of the non-doped zirconia prepared using the same method (130 $m^2\ g^{-1}$, ref. 19). This stabilizing effect of a polyvalent oxoanion on the zirconia dispersions seems to be a general phenomenon, described earlier for molybdate and sulfate.[25]

For the ratios of P/Zr = 0.3 or 1 (samples 2, 6), narrow lines of crystalline K–Zr phosphates appeared, the solids being present as mixtures of different ternary phosphates with dispersed zirconia. These samples are not homogeneous because of a P/Zr ratio insufficient to produce any pure compounds. Specific surfaces are intermediate between those of doped zirconia (P/Zr = 0.1) and crystalline phosphates.

Pure ternary compounds can be obtained at the ratios P/Zr $\geqslant$ 4. In this case the reaction temperature determines the nature of the product. NASICON is the only product at 350 °C whatever the duration of the reaction (Fig. 9). The layered phase was obtained at 500 °C but it contained some NASICON impurity. To prepare the pure layered compound, the reaction temperature should be increased to 550 °C.

^{31}P NMR

MAS ^{31}P spectra with proton decoupling of the samples 4, 5 and 10 are presented in Fig. 10, showing characteristic bands of the NASICON phase in the sample 4 (δ −24.9) and layered

Table 1 Chemical composition, XRD phases and specific surface area (S) of the solids as a function of temperature and P/Zr ratio in the melt

no	T/°C	P/Zr	composition	phases (XRD)	S/m^2 g^{-1}
1	350	0.1	$K_{0.03}Zr(PO_4)_{0.078}$	ZrO_2: broad lines	116
2	350	0.3	$K_{0.11}Zr(PO_4)_{0.3}$	ZrO_2 + NASICON	58
3	350	1	$K_{0.24}Zr(PO_4)_{0.69}$	NASICON + ZrO_2	30
4	350	10	$K_{1.00}Zr_2(PO_4)_{3.00}$	NASICON	5
5	500	0.1	$K_{0.06}Zr(PO_4)_{0.09}$	ZrO_2(T)	200
6	500	1	$K_{0.31}Zr(PO_4)_{0.88}$	ZrO_2 + layered + NASICON	70
7	500	4	$K_{1.91}Zr(PO_4)_{1.94}$	layered + NASICON	15
8	500	10	$K_{1.94}Zr(PO_4)_{1.96}$	layered + NASICON (traces)	17
9	500[a]	4	$K_{1.99}Zr(PO_4)_{1.98}$	layered + NASICON (traces)	15
10	550[a]	4	$K_{2.01}Zr(PO_4)_{2.02}$	layered	12
11	270	4	$K_{0.93}Zr_2(PO_4)_{2.78}$	$KHZr(PO_4)_2$ + KPO_3	—

[a]Duration of reaction is 20 h.

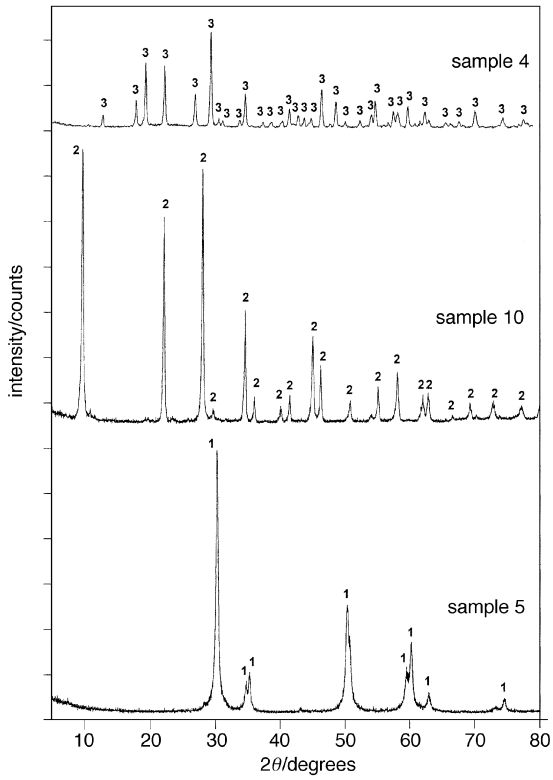

Fig. 9 XRD patterns of the selected samples from Table 1. Peaks 1, ZrO_2 (JCPDS 14-0534); 2, $KZr_2(PO_4)_3$ (JCPDS 35-0756); 3, $K_2Zr(PO_4)_2$ (ref. 23).

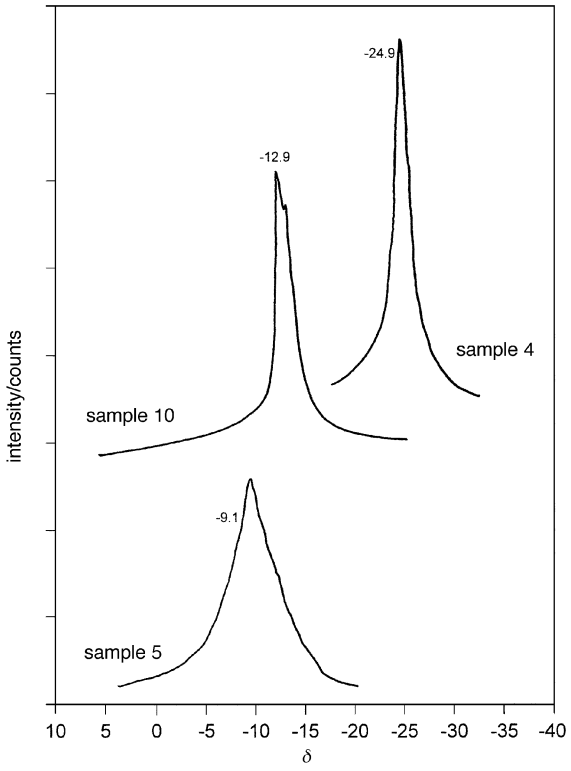

Fig. 10 ^{31}P MAS NMR spectra of selected samples from Table 1

phosphate in the sample 10 (δ −12.9). The sample 5, prepared at P/Zr = 0.1 and consisting of the phosphate-modified tetragonal ZrO_2 phase, showed a single broad band at δ −9.12. Since in this sample the phosphate groups are anchored on a heterogeneous surface of zirconium oxide, the resonance band is broadened.

In the earlier works,[26] the chemical shift of ^{31}P in the orthophosphates was related to the electronegativity of the next-neighbour cations, so that the progressive decrease of the environment electronegativity leads to the increase of the chemical shift. Therefore, replacing the Zr coordinating a phosphate group with a K^+ ion should increase the value of δ. For the anhydrous orthophosphates containing only one cation and no other anions than orthophosphate, the chemical shift was expressed in the form: $\delta(\text{ppm}) = -35.5(\text{EN}) + 41$, where EN is the Pauling electronegativity of the cation.

For the solids studied here the second coordination shell of ^{31}P can include K, Zr and H. We tried to find a correlation between the composition of the solids prepared in this work (and some lit. references) and the isotropic chemical shift of ^{31}P. Excluding from consideration any proton-containing solids, a quite good correlation could be obtained between the chemical shift of phosphorus and the mean electronegativity χ of the solid, calculated according to eqn. (12),[27]

$$\chi = [\sum_i (\chi^*_i)^{1/2} + 1.36z]/\sum_i (\chi^*_i)^{-1/2} \quad (12)$$

where χ^*_i are the electronegativities of the constituent elements and z is the total charge of a chemical entity.

The linear dependence of the chemical shift on the mean electronegativity obeys the formula $\delta(\text{ppm}) = 117 - 54\chi$, with a correlation coefficient of 0.997 for the points indicated in Fig. 11. Although being satisfactory for the points selected, the above relation is of course of no general value, because both hydrogen-containing solids and those with several different phosphorous species in the structure cannot be described by this relation.

^{1}H NMR

The spectra were obtained after heating the samples in a vacuum oven at 120 °C overnight to remove as much of the absorbed water as possible. However, since the spectra were obtained in air, a large signal of adsorbed water at δ *ca.* 4.7 was found in all the products. This was the only signal for the sample 5 (consisting of phosphate-modified zirconia). Apart from the adsorbed water, three narrow bands have been found

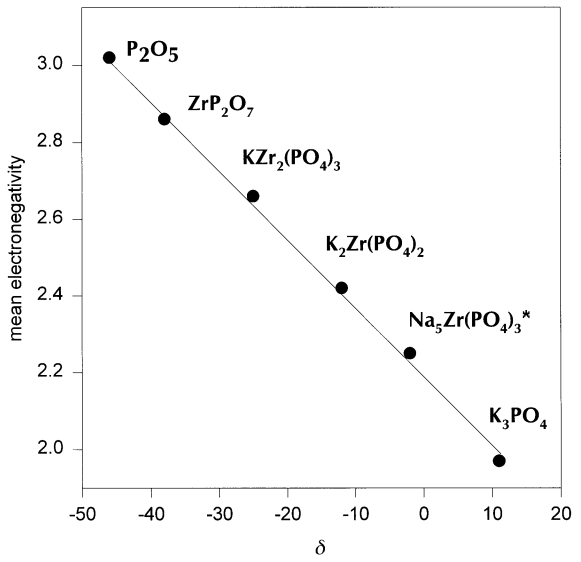

Fig. 11 Correlation between the isotropic chemical shifts of some Zr compounds and their mean electronegativities. *, value taken from ref. 30.

at δ 3.27, 1.95 and 9.98 in the other samples (Fig. 12). The observation of these peaks is well correlated with the presence of $K_2Zr(PO_4)_2$ (δ 3.27) and $KZr_2(PO_4)_4$ (δ 1.95 and 9.98) in the solids studied. Only one line is attributed to the layered phase, whereas there are two peaks for NASICON, according to the number of chemically different cationic sites in their structures,[28] which probably can be partially occupied by protons. Since the chemical shift of protons is correlated to the Brønsted acidity of a solid, it can be stated that layered K–Zr phosphate provides only one type of basic OH group whereas in the case of the NASICON phase a bimodal distribution is observed with the presence of both basic and acidic OH groups. The acid–base properties of zirconium phosphates may be of eminent importance for their catalytic properties, either in the case of alkali- or transition-metal exchanged phosphates.[15,29]

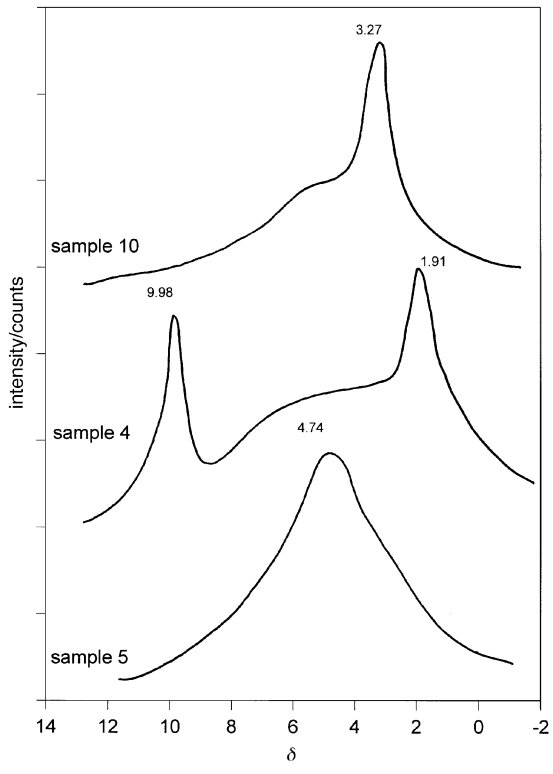

Fig. 12 ^{1}H MAS NMR spectra of selected samples from Table 1

As follows from our preliminary unpublished data, the molten salt preparations of NASICON and/or layered phases can be easily modified with other chemical elements, by means of doping the melts with anionic (for example, chromate or vanadate) or cationic (iron, nickel) species. Therefore, the molten salt technique provides a flexible way for the preparation of dispersed mixed phases, containing different oxoanions and (transition)-metal cations, which may present great interest for catalysis and other applications.

Conclusions

Dispersed solids including phosphate-modified zirconia and mixed K–Zr phosphates can be prepared by means of reactions of hydrated $ZrOCl_2$ and $NH_4H_2PO_4$ salts with KNO_3 in the temperature range 250–550 °C. Individual phases of $KZr_2(PO_4)_3$ with NASICON structure, or layered $K_2Zr(PO_4)_2$ are precipitated in the melt in certain temperature ranges. Though the reaction occurs in the nitrate melt, its mechanism seems to be that of a metathetical exchange rather than that of a Lux–Flood acid–base interaction. The reactivity of the melt increases with the temperature, leading to products enriched in potassium and phosphorus.

References

1 D. Hamon, M. Vrinat, M. Breysse, B. Durand, M. Jebrouni, M. Robin, P. Magnoux and T. des Courieres, *Catal. Today*, 1991, **10**, 613.
2 E. Kulikova, J. P. Deloume, L. Mozoni, B. Durand and M. Vrinat, *Eur. J. Solid State Inorg. Chem.*, 1994, **31**, 487.
3 Y. Du and D. Inman, *J. Mater. Chem.*, 1996, **6**, 1239.
4 P. Afanasiev, C. Geantet and M. Breysse, *J. Catal.*, 1995, **153**, 17.
5 D. A. Habboush and D. H. Kerridge, *Thermochim. Acta*, 1974, **10**, 187.
6 J. L. Copeland and L. Gutierrez, *J. Phys. Chem.*, 1973, **77**, 20.
7 J. L. Copeland, A. S. Metcalf and B. R. Hubble, *J. Phys. Chem.*, 1976, **80**, 236.
8 A. Baraka, A. J. Abdel-Rohman and E. A. El-Taher, *J. Electroanal. Chem.*, 1984, **164**, 273.
9 S. Allulli and G. Cardini, *J. Inorg. Nucl. Chem.*, 1972, **34**, 339.
10 S. Allulli, A. La Ginestra and N. Tomassini, *J. Inorg. Nucl. Chem.*, 1984, **36**, 3839.
11 S. Allulli, N. Tomassini and M. A. Massucci, *J. Chem. Soc., Dalton Trans.*, 1976, 1816.
12 A. Clearfield in, *Inorganic Ion Exchange Materials*, ed. A. Clearfield, CRC Press, Boca Raton, FL, 1982, p. 1.
13 J. B. Goodenough, H. Y. P. Hong and J. A. Kafalas, *Mater. Res. Bull.*, 1976, **11**, 203.
14 J. B. Moffat, *Catal. Rev. Sci. Eng.*, 1978, **18**, 199.
15 S. Arsalane, M. Ziyad, G. Coudurier and J. C. Vedrine, *J. Catal.*, 1996, **159**, 162.
16 M. E. Hagerman and K. R. Poppelmeier, *Chem. Mater.*, 1995, **7**, 602.
17 P. Afanasiev and C. Geantet, *C. R. Acad. Sci. Paris*, 1993, **317**(II), 601.
18 W. Kraus and G. Nolze, Powder Cell 1.8 program, 1995.
19 P. Afanasiev and C. Geantet, *Mater. Chem. Phys.*, 1995, **41**, 18.
20 P. Afanasiev, C. Geantet, M. Lacroix and M. Breysse, *J. Catal.*, 1996, **162**, 143.
21 Y. Sadaoka, Y. Sakai and M. Matsuguchi, *J. Mater. Sci.*, 1989, **24**, 2081.
22 A. Clearfield, P. Jirustithipong, R. N. Cotman and S. P. Pack, *Mater. Res. Bull.*, 1980, **15**, 1603.
23 N. S. Slobodyanik, P. G. Nagornyi, Z. I. Kornienko and E. S. Lugovskaya, *Russ. J. Inorg. Chem.*, 1988, **33**, 247.
24 M. Dorffel and J. Liebertz, *Z. Kristallogr.*, 1990, **193**, 155.
25 P. Afanasiev, C. Geantet and M. Breysse, *J. Mater. Chem.*, 1994, **4**, 1653.
26 G. L. Turner, K. A. Smith, R. J. Kirkpatrick and E. Oldfield, *J. Magn. Reson.*, 1986, **70**, 408.
27 J. Livage, M. Henry and C. Sanchez, *Prog. Solid State Chem.*, 1988, **18**, 259.
28 L. O. Hagman and P. Kierkegaard, *Acta Chem. Scand.*, 1968, **22**, 182.
29 A. Serghini, M. Kacimi, M. Ziyad and R. Brochu, *J. Chim. Phys.*, 1988, **85**, 499.
30 K. C. Sobha and K. J. Rao, *J. Solid State Chem.*, 1996, **121**, 197.

Paper 6/07068J; *Received* 16*th October*, 1996